

Survival Analysis with Adversarial Regularization

Michael Potter

Electrical and Computer Engineering
Northeastern University
Boston, USA
potter.mi@northeastern.edu

Stefano Maxenti

Electrical and Computer Engineering
Northeastern University
Boston, USA
maxenti.s@northeastern.edu

Michael Everett

Electrical and Computer Engineering
Northeastern University
Boston, USA
m.everett@northeastern.edu

Abstract—Survival Analysis (SA) models the time until an event occurs, with applications in fields like medicine, defense, finance, and aerospace. Recent work shows that Neural Networks (NNs) can capture complex relationships in SA. However, dataset uncertainties (e.g., noisy measurements, human error) can degrade model performance. To address this, we leverage NN verification advances to create algorithms for robust, fully-parametric survival models. We introduce a robust loss function and use CROWN-IBP regularization to handle computational challenges in the Min-Max problem. Evaluating our approach on SurvSet datasets, we find that our Survival Analysis with Adversarial Regularization (SAWAR) method consistently outperforms baselines under various perturbations with respect to Negative Log Likelihood (NegLL), Integrated Brier Score (IBS), and Concordance Index (CI). This demonstrates that adversarial regularization enhances SA performance and calibration, mitigating data uncertainty and improving generalization across diverse datasets up to 150% across all perturbation magnitudes.

Code: <https://github.com/mlpotter/SAWAR>

Index Terms—Survival Analysis, Adversarial Robustness, Neural Networks, Calibration, CROWN-IBP, Cox-Weibull

I. INTRODUCTION

SURVIVAL Analysis (SA) models the time until an event occurs and has extensive applications. For example, SA has been used extensively in medicine for evaluating treatments in cancer patients and drug trials [1]. Early methods relied on linear parametric models [2], but recent advancements utilize Neural Networks (NNs) to handle complex time-to-event data [3].

A major challenge in Survival Analysis (SA) is developing models robust to dataset uncertainty and variability. This is particularly essential for clinical applications where treatment efficacy must be demonstrated across diverse patient demographics, institutions, and data acquisition settings [4]–[6]. Data uncertainty can arise from human errors, such as poor handwriting by physicians [7] and ineffective medical record-keeping [8], as well as inherent noise during data collection [9]. Many approaches assume perfect measurement of covariates, neglecting aleatoric uncertainty [10], which in SA is associated with noise in the log of measured time-to-event [11]. Further, adversaries can manipulate data to make models

over- or under-confident [12]. Despite these issues and the sensitivity of NNs to input uncertainties, robustness techniques against data perturbations in SA remains underexplored.

To address these issues, this paper’s contributions include:

- Survival Analysis with Adversarial Regularization (SAWAR) for training robust, fully-parametric, NN-based SA models using adversarial covariate perturbations and convex relaxations, enhancing model calibration and stability against noisy data.
- Experiments demonstrating the sensitivity of existing NN-based SA methods to covariate perturbations across 10 publicly available medical SA datasets, highlighting an area for improvement in the current state of the art.

II. RELATED WORK

This section reviews NN literature for SA, with more details in [13]. The first use of NNs in SA was a shallow Feedforward Neural Network (FFNN) to approximate the survival function [14]. Later, deeper models were developed, such as Cox-nnet [15], a NN for Cox Proportional Hazard (CPH) modeling [11]. Building on this, DeepSurv [16] introduced a CPH NN with dropout layers for better generalization in personalized treatment. Then, mixture models such as DeepWeiSurv [17] further advanced the field by using NNs to regress Weibull mixture distribution parameters. These methods enhance modeling capability but do not always improve model calibration and robustness.

Recent works focus on improving model calibration [18]–[20], which ensures predicted confidence matches true likelihood [21]. However, few works address adversarial robustness in SA, where small input perturbations should not mislead the model [22]. Although better calibration does not always enhance generalization [23], integrating adversarial robustness improves model trustworthiness in calibration and stability on unexpected data [24].

Existing adversarial training methods for SA involve trade-offs between model complexity, performance, and incorporating physical assumptions. Most techniques use Conditional Generative Adversarial Networks (CGANs) to generate time-to-event samples from a survival distribution non-parametrically [25]–[27]. These models implicitly define the survival distribution without assuming a functional/analytical form, offering increased flexibility to fit various data realizations [28]–[30]. However, this flexibility can violate Bayesian

Occam’s Razor, which penalizes overly complex models [30]. To balance complexity and performance, inductive biases are used in explicit parametric models [29]. One common bias in SA is the memoryless property, satisfied by the exponential distribution [28]. Thus, this paper employs the exponential CPH model, widely used in SA [31]–[33], as well as in queuing theory [34], reliability analysis [3], and telecommunications [35].

III. PRELIMINARIES ON SURVIVAL ANALYSIS

SA [11] is a statistical approach used to analyze and model the time $t \in \mathcal{R}_{++}$ until an event $e \in \{0, 1\}$ happens (e.g., a disease occurs, a device breaks). Typically, the study happens over a finite time period and instances/individuals may leave the study early before an event is recorded, with no follow up. In those cases, the dataset records that no event occurred up until the exit time of the study, which is called *right censoring* [36]. Such an SA dataset consists of N independent instances/individuals, each denoted by index i , for which time between entry to a study and the subsequent event is recorded. Upon entry time to a study, each instance’s *covariates* $\mathbf{x}_i \in \mathcal{R}^d$ (i.e., variables that may affect the event of interest for the study) are measured. In summary, the dataset \mathcal{D} has the following structure:

$$\mathcal{D} = \{(\mathbf{x}_i, t_i, e_i)\}_{i=1}^N. \quad (1)$$

Being a statistical approach, we define the required probabilistic functions to model time-to-event data next.

A. Cox Proportional Hazard Model

Let us denote T as a continuous, non-negative, random variable that represents the time-to-event, with Probability Density Function (PDF) $f(t)$ and Cumulative Distribution Function (CDF) $F(t) = P[T \leq t]$. The survival function $S(t) := 1 - F(t)$ is the complement of this CDF [11], [37].

An exponential parametric survival model is expressed as

$$S(t) = e^{-\Lambda(t)}, \quad (2)$$

where $\Lambda(t) = \int_0^t \lambda(u)du$ is the cumulative hazard and

$$\lambda(t) = \frac{f(t)}{S(t)} = \lim_{\Delta \rightarrow 0} \frac{P[t < T < t + \Delta]}{\Delta} \quad (3)$$

is the instantaneous failure rate at time t .

To incorporate the instance’s covariates, we use the prevalent CPH model [2]:

$$\lambda_{\theta}(t, \mathbf{x}) = \lambda_0(t)e^{G_{\theta}(\mathbf{x})}, \quad (4)$$

where $\lambda_0(t)$ is a baseline hazard, $e^{G_{\theta}(\mathbf{x})}$ is the relative risk associated with covariates \mathbf{x} , and $G_{\theta}(\mathbf{x})$ is an NN with parameters θ in our setting.

The exponential CPH model characterizes the baseline hazard rate as $\lambda_0(t) = \lambda_0$. For simplicity, we assume an exponential baseline hazard and “absorb” the λ term into the bias of the NN:

$$\lambda_0 e^{G_{\theta}(\mathbf{x})} = e^{\log \lambda_0 + G_{\theta}(\mathbf{x})} = e^{G_{\theta}(\mathbf{x})}. \quad (5)$$

The exponential CPH model’s PDF, CDF, and complement CDF are $f_{\theta}(t|\mathbf{x}) = e^{G_{\theta}(\mathbf{x})}e^{-e^{G_{\theta}(\mathbf{x})}t}$, $F_{\theta}(t|\mathbf{x}) = 1.0 - e^{-e^{G_{\theta}(\mathbf{x})}t}$, $S_{\theta}(t|\mathbf{x}) = e^{-e^{G_{\theta}(\mathbf{x})}t}$, respectively. $S_{\theta}(t|\mathbf{x})$ is also known as the *instance survival function*.

The *population survival curve* is the marginalization of the instance survival function over the covariates,

$$S(t) = \int S_{\theta}(t|\mathbf{x})p(\mathbf{x})d\mathbf{x}. \quad (6)$$

Since the distribution of the covariates $p(\mathbf{x})$ is typically unknown, the integral in Eq. (6) is often replaced with a Monte Carlo estimate [18]:

$$S(t) \approx \frac{1}{N} \sum_{i=1}^N S_{\theta}(t|\mathbf{x}_i). \quad (7)$$

Given these definitions, the next section describes the baseline objective for finding model parameters θ from dataset \mathcal{D} .

B. Baseline Objective Functions

We follow [25], [38] to define two objective functions based on negative log likelihood (Section III-B1) and the rank correlation (Section III-B2).

1) *Right Censored Log Likelihood Objective*: The \mathcal{L}_{LL} objective is the log of the time-to-event likelihood over \mathcal{D} specified by the CPH model [11]:

$$\mathcal{L}_{LL}(\theta; \mathbf{X}, \mathbf{t}, \mathbf{e}) = \sum_{i=1}^N e_i \cdot \log f_{\theta}(t_i|\mathbf{x}_i) + \sum_{i=1}^N (1 - e_i) \cdot \log S_{\theta}(t_i|\mathbf{x}_i). \quad (8)$$

The first summation in Eq. (8) is the log likelihood of the datapoints corresponding to when the event occurs and the exact time of occurrence is observed. The second summation in Eq. (8) is the log likelihood when right censoring occurs.

2) *Ranking Objective*: The \mathcal{L}_{rank} objective is a ranking loss that penalizes an incorrect ordering of pairs $\{F_{\theta}(t_i|\mathbf{x}_i), F_{\theta}(t_j|\mathbf{x}_j)\}$, where instance i with event time $t_i < t_j$ should have a higher probability of failure than instance j at time t_i :

$$\mathcal{L}_{rank}(\theta; \mathbf{X}, \mathbf{t}, \mathbf{e}) = \sum_{i \neq j} A_{i,j} \eta \left(F_{\theta}(t_i|\mathbf{x}_i), F_{\theta}(t_j|\mathbf{x}_j) \right), \quad (9)$$

where $\eta(\mathbf{x}, \mathbf{y}) = \exp\left(-\frac{(\mathbf{x}-\mathbf{y})}{\sigma}\right)$ and $A_{i,j}$ indicates an “acceptable” comparison pair [38], [39]. We set $\sigma = 1$ for all experiments.

3) *Combined Objective*: The combined right censored negative log likelihood objective and the risk ranking objective, with risk ranking objective weight trade-off $w = \frac{1}{\text{batch_size}}$, is

$$\mathcal{L}(\theta; \mathbf{X}, \mathbf{t}, \mathbf{e}) = -\mathcal{L}_{LL}(\theta; \mathbf{X}, \mathbf{t}, \mathbf{e}) + w \cdot \mathcal{L}_{rank}(\theta; \mathbf{X}, \mathbf{t}, \mathbf{e}). \quad (10)$$

This combined objective provides a trade-off between finding the NN parameters θ that maximize the likelihood of observing \mathcal{D} and maximize a rank correlation between the instance

risk scores and the observed failure times. We will denote the combined loss as the *baseline* objective. Our baseline model’s objective is similar to Deep Regularized Accelerated Failure Time (DRAFT) [25] but with a different ranking objective function. Thus, we consider the baseline training method for robust SA baseline method as DRAFT.

Thus far, we have described an objective function that improves predictive performance:

$$\theta^* = \arg \min_{\theta} \mathcal{L}(\theta; \mathbf{X}, \mathbf{t}, e). \quad (11)$$

In the following sections, we address how to develop NN models that are robust against adversarial perturbations.

IV. PRELIMINARIES ON ADVERSARIAL TRAINING

Adversarial training [22], [40], [41] improves robustness and generalization of NNs to uncertain data. Rather than training on pristine data, most adversarial training approaches perturb the data throughout the training process to encourage the model to optimize for parameters that are resilient against such perturbations. For example, [42] formulated adversarial training as solving a Min-Max robust optimization problem:

$$\min_{\theta} \max_{\tilde{\mathbf{X}}} \mathcal{L}(\theta; \tilde{\mathbf{X}}), \quad (12)$$

where $\tilde{\mathbf{X}} = \{\tilde{\mathbf{x}}_i \in \mathcal{B}(\mathbf{x}_i, \epsilon)\}_{i=1}^N$, and $\mathcal{B}(\mathbf{x}_i, \epsilon)$ is the ℓ_{∞} -ball of radius ϵ around \mathbf{x}_i .

In practice, the Min-Max problem posed in [42] is intractable to compute exactly. In particular, the inner maximization requires finding a global optimum over a high dimensional and non-convex loss function over NN parameters. Therefore, many recent adversarial training methods propose approximations to Eq. (12), leading to models with varying degrees of robustness to different data uncertainties. To understand the robustness properties of SA models to a variety of data uncertainties present in real applications, this paper investigates several perturbation methods, described next.

A. Certifiable Robustness

One such approximation is to use techniques from NN verification during training. For example, CROWN-Interval Bound Propagation (CROWN-IBP) combines CROWN and Interval Bound Propagation (IBP) methods to obtain a convex relaxation for the lower bound and upper bound of each layer in the NN with respect to input data [40], [43]. CROWN-IBP is commonly used for verifying NN properties over a range of possible inputs. [40], [44] showed the linear relaxation can be extended to the entire objective function:

$$\max_{\tilde{\mathbf{X}}} \mathcal{L}(\tilde{\mathbf{X}}) \leq \bar{\mathcal{L}}(\tilde{\mathbf{X}}). \quad (13)$$

This relaxation is convex with respect to NN weights, enabling efficient optimization, and by optimizing over an upper bound on the inner maximization, it accounts for a strong adversary during training.

B. Adversarial Perturbations

Another way to approximate Eq. (20) is to use adversarial perturbations. Whereas CROWN-IBP provides an upper bound on the inner maximization (i.e., $\max_{\tilde{\mathbf{X}}} \mathcal{L}(\theta; \tilde{\mathbf{X}})$), adversarial perturbation algorithms typically provide a lower bound:

$$\max_{\tilde{\mathbf{X}}} \mathcal{L}(\theta; \tilde{\mathbf{X}}) \geq \mathcal{L}(\theta; \tilde{\mathbf{X}}_{FGSM}). \quad (14)$$

Fast Gradient Sign Method (FGSM) [45] uses the gradient of the objective function with respect to the input \mathbf{x} to perturb \mathbf{x} in the direction that maximizes the objective \mathcal{L} . Projected Gradient Descent (PGD) [42] iteratively applies that same type of first-order perturbation K times (or until convergence is reached), but constrains the perturbation of \mathbf{x} to remain within a specified set (e.g., ℓ_p -ball). FGSM is a special case of PGD, with $K = 1$ and the ℓ_{∞} -ball.

Considering the structure of the datasets as described in Section III, we perturb only the covariates \mathbf{x} and not the time-to-event t . The perturbed covariates are calculated as:

$$\mathbf{x}^{(0)} = \mathbf{x}, \quad (15)$$

$$\mathbf{x}^{(k+1)} = \Pi_{\mathcal{B}(\mathbf{x}, \epsilon)} \left(\mathbf{x}^{(k)} + \alpha (\nabla_{\mathbf{x}} \mathcal{L}(\theta; \mathbf{x}^{(k)}, \mathbf{t}, e)) \right), \quad (16)$$

$$\tilde{\mathbf{x}} = \mathbf{x}^{(K)}, \quad (17)$$

where k is the iteration step and α is a step size parameter.

C. Random Noise

While robustness to a worst-case perturbation is important for many applications, adding random noise to training data has also been shown to improve generalization performance [46]. Therefore, this paper also considers Gaussian Noise perturbations with variance ϵ bounded within an ℓ_{∞} -ball:

$$\mathbf{z} \sim \mathcal{N}(0, \mathbf{I}), \quad (18)$$

$$\tilde{\mathbf{x}} = \mathbf{x} + \Pi_{\mathcal{B}(0, \epsilon)}(\sqrt{\epsilon} \mathbf{I} \mathbf{z}). \quad (19)$$

Building on this foundation, we next introduce our approach, SAWAR, that develops robust SA models based on adversarial regularization.

V. SURVIVAL ANALYSIS WITH ADVERSARIAL REGULARIZATION

This paper addresses the open challenge in SA of developing models robust to dataset uncertainty and variability, as motivated in Section I. We propose a method for adversarial robustness in fully-parametric NN-based SA, enhancing calibration and stability on unexpected or noisy data. Our approach extends the objective function (Eq. (10)) with adversarial regularization as a Min-Max optimization problem (Eq. (12)) [40], [41], as detailed in the following sections.

A. Min-Max Formulation

When solving for θ in SA, many approaches treat each measurement in dataset \mathcal{D} as ground-truth, ignoring aleatoric uncertainty [10]. Typically in SA, the aleatoric uncertainty is only associated with the noise of the log of the measured time-to-event (e.g. the Gumbel distribution or Log Normal

distribution) [11]. Instead, the proposed SAWAR approach assumes that each covariate is subject to a perturbation within a bounded uncertainty set, which leads to a robust optimization formulation as in Section IV. Thus, we optimize the NN parameters for the worst-case realizations of Eq. (10):

$$\min_{\theta} \max_{\tilde{\mathbf{X}}} \mathcal{L}(\theta; \tilde{\mathbf{X}}, \mathbf{t}, \mathbf{e}). \quad (20)$$

We use the open-source, PyTorch-based library `auto_LiRPA` [44] to compute the CROWN-IBP upper bound to the inner maximization term in Eq. (20), which is fully differentiable for backpropagation.

B. Adversarial Robustness Regularization

[41] shows that tight relaxations to the inner maximization of a Min-Max problem can over-regularize the NN, leading to poor predictive performance. Therefore, we balance the objective in Eq. (10) with the adversarial robustness objective in Eq. (20) [40], [43] to combine predictive performance and adversarial robustness as:

$$\min_{\theta} \left[\kappa \cdot \mathcal{L}(\theta; \mathbf{X}, \mathbf{t}, \mathbf{e}) + (1 - \kappa) \cdot \max_{\tilde{\mathbf{X}}} \mathcal{L}(\theta; \tilde{\mathbf{X}}, \mathbf{t}, \mathbf{e}) \right], \quad (21)$$

where $\kappa \in (0, 1)$.

C. SAWAR Training

The NN parameters are updated using stochastic gradient descent with the ADAM optimizer [47], where we use early stopping [48] with respect to the validation set to prevent overfitting. We introduce the covariate perturbations after 100 epochs. A smooth ϵ -scheduler linearly increases the ϵ -perturbation magnitude from 0.0 to 0.5 within a 30 epoch window after 100 epochs. We do not allow early stopping until after the maximum ϵ -perturbation magnitude is achieved.

We expect that the model’s adversarial robustness and predictive calibration should increase when incorporating data uncertainty in SAWAR objective [24] via the adversarial regularization term in Eq. (21) and show SAWAR’s improved performance via extensive experiments in the next section.

VI. EXPERIMENTS

We conduct experiments over 10 benchmark medical SA datasets (VI-B) to quantify the impact of perturbation after the robust training is complete. As evaluation metrics, we consider the Concordance Index (CI) [49], the Integrated Brier Score (IBS) [50] and the Negative Log Likelihood (NegLL) at varying ϵ -perturbation magnitudes from 0 to 1. To demonstrate that SAWAR produces SA models that perform well and are robust to dataset uncertainty, this section quantifies the improvement in predictive accuracy, calibration, and population curve estimation.

A. Configuration

The experiments are conducted on a Windows computer with a 12th Gen Intel(R) Core (TM) i9-12900 processor and 16 GB RAM. Each dataset undergoes stratified partitioning into train, validation, test sets with proportions 60%, 20%, 20%

respectively. The NN G_{θ} has 2 hidden layers of 50 neurons each and *Leaky ReLU* activation functions. We use *lifelines* [51] and *sksurv* [39] for computing SA metrics.

B. Datasets

We use the API *SurvSet* [52] to download the benchmark medical SA datasets shown in Table I and described below:

Dataset	N	n_{fac}	n_{ohe}	n_{num}
TRACE	1878	4	4	2
stagec	146	4	15	3
flchain	7874	4	26	6
Aids2	2839	3	11	1
Framingham	4699	2	12	5
dataDIVAT1	5943	3	14	2
prostate	502	6	16	9
zinc	431	11	18	2
retinopathy	394	5	9	2
LeukSurv	1043	2	24	5

TABLE I: Studied datasets from *SurvSet*. n_{fac} is the number of categorical features, n_{ohe} is number of binary features (one-hot-encoded) and n_{num} is number of numerical features.

- 1) The **TRACE** [53] dataset is from a study on a subset of patients admitted after myocardial infarction to examine various risk factors.
- 2) The **stagec** [54] dataset is from a study exploring the prognostic value of flow cytometry for patients with stage C prostate cancer.
- 3) The **flchain** [55] dataset is from a study on the relationship between serum free light chain (FLC) and mortality of Olmsted Country residents aged 50 years or more.
- 4) The **Aids2** [56] dataset is from patients diagnosed with AIDS in Australia before 1 July 1991.
- 5) The **Framingham** [57] dataset is from the first prospective study of cardiovascular disease with identification of risk factors and joint effects.
- 6) The **dataDIVAT1** [58] dataset is from the first sample from the DIVAT Data Bank for French kidney transplant recipients from DIVAT cohort.
- 7) The **prostate** [59] dataset is from a randomised clinical trial comparing treatment for patients with stage 3 and stage 4 prostate cancer.
- 8) The **zinc** [60] is from the first study to examine association between tissue elemental zinc levels and the esophageal squamous cell carcinoma.
- 9) The **retinopathy** [61] is from the trial of laser coagulation as treatment to delay diabetic retinopathy.
- 10) The **LeukSurv** [62] is from the study on survival of acute myeloid leukemia and connection to spatial variation in survival.

We preprocess each dataset by one-hot encoding categorical covariates and standard normalization of all covariates.

C. Adversary Setup

We apply two adversarial perturbation settings on the test set to assess the robustness of the proposed adversarial regularization method: FGSM perturbation (Section IV-B) and a novel worst-case perturbation. FGSM is applied by using the

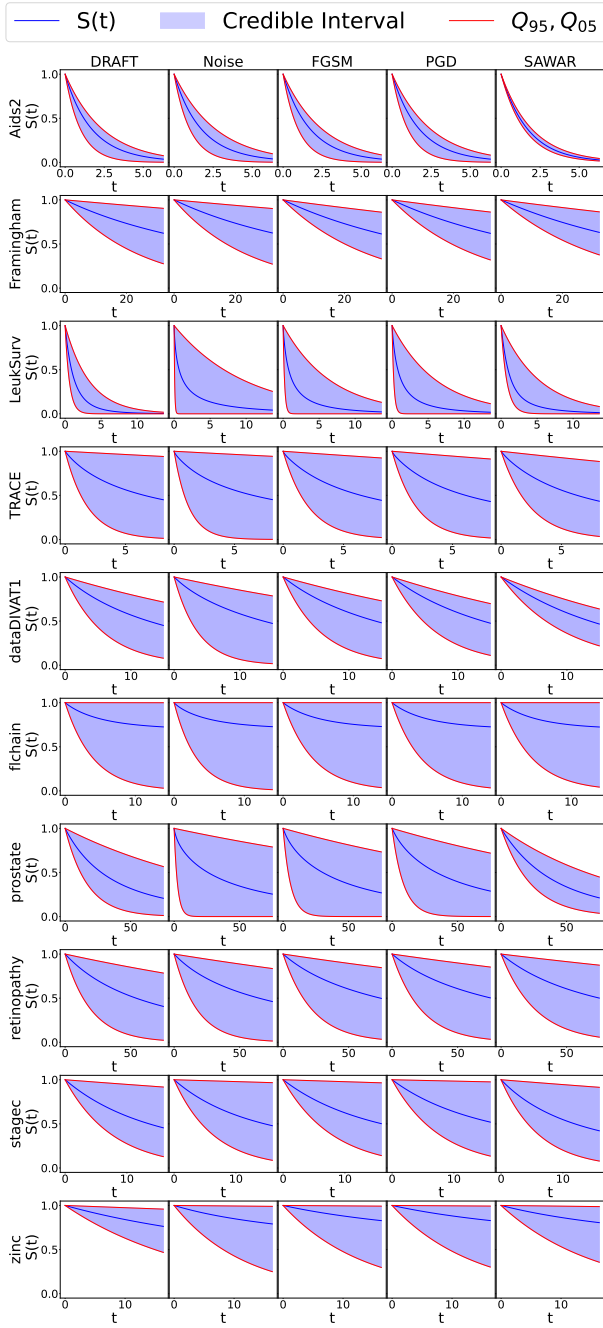


Fig. 1: Distribution of survival curves for DRAFT, FGSM, PGD, and CROWN-IBP. As the strength of the adversarial training method increases, from left to right column, the 90% credible interval narrows. However, the credible interval of SAWAR does not drastically differ from the DRAFT.

gradient of the objective function with respect to the input \mathbf{x} to perturb \mathbf{x} in the direction that maximizes the objective Eq. (20), such that:

$$\tilde{\lambda}_{\theta} = e^{G_{\theta}(\text{FGSM}(\mathcal{L}, \mathbf{x}))}. \quad (22)$$

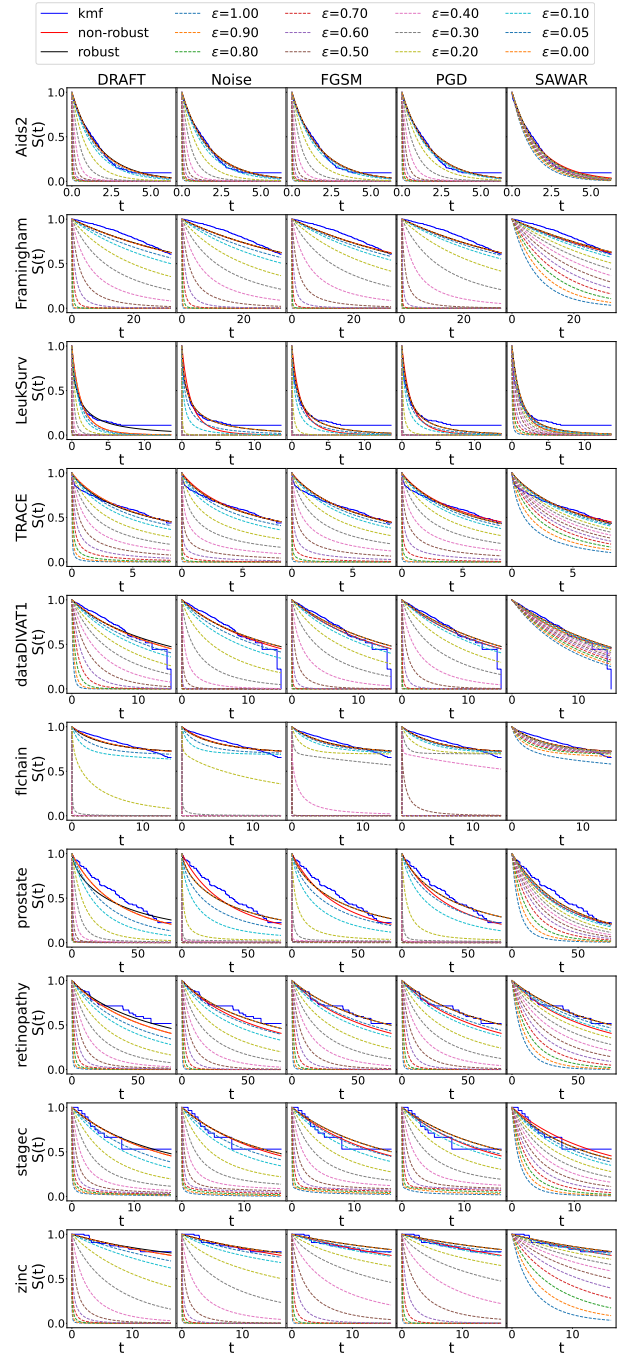


Fig. 2: Adversarial robustness of survival curves for DRAFT, FGSM, PGD, and CROWN-IBP training against ϵ -worst-case perturbation. As the strength of the adversarial training method increases, from left to right column, the perturbed population survival curve for a given ϵ is closer to the KMC.

We define the worst-case perturbation as the maximum failure rate with respect to the covariate uncertainty:

$$\tilde{\lambda}_{\theta} = \max_{\tilde{\mathbf{x}}_i \in \mathcal{B}(\mathbf{x}_i, \epsilon)} e^{G_{\theta}(\tilde{\mathbf{x}}_i)}, \quad (23)$$

and the ϵ -worst-case survival curve as the lowest survival probability at a given time t with respect to the ϵ -perturbed

ϵ	Concordance Index					Integrated Brier Score					Negative Log Likelihood				
	DRAFT	Noise	FGSM	PGD	SAWAR	DRAFT	Noise	FGSM	PGD	SAWAR	DRAFT	Noise	FGSM	PGD	SAWAR
1.00	<u>2.9</u>	3.35	3.35	2.5	<u>2.9</u>	4.6	4.4	2.4	<u>1.9</u>	1.7	4.0	4.7	2.7	<u>2.1</u>	1.5
0.90	3.1	3.5	3.45	2.45	<u>2.5</u>	4.5	4.5	2.5	<u>1.8</u>	1.7	4.0	4.7	2.9	<u>1.9</u>	1.5
0.80	3.4	3.4	3.2	2.35	<u>2.65</u>	4.6	4.4	2.6	<u>1.8</u>	1.6	4.1	4.6	3.0	<u>1.9</u>	1.4
0.70	3.45	3.35	3.1	2.4	<u>2.7</u>	4.7	4.3	2.6	<u>1.8</u>	1.6	4.2	4.5	3.0	<u>2.0</u>	1.3
0.60	3.45	3.45	3.0	2.5	<u>2.6</u>	4.7	4.3	2.7	<u>1.8</u>	1.5	4.2	4.5	3.1	<u>2.1</u>	1.1
0.50	3.85	3.65	3.1	2.1	<u>2.3</u>	4.4	4.6	2.9	<u>1.8</u>	1.3	4.1	4.5	3.2	<u>2.1</u>	1.1
0.40	3.9	3.8	3.05	2.1	<u>2.15</u>	4.4	4.6	3.0	<u>1.9</u>	1.1	4.0	4.6	3.2	<u>2.1</u>	1.1
0.30	4.4	4.2	3.0	1.9	1.5	4.4	4.6	3.0	<u>1.9</u>	1.1	4.0	4.6	3.2	<u>2.1</u>	1.1
0.20	4.35	4.0	3.3	<u>2.25</u>	1.1	4.2	4.6	3.2	<u>2.0</u>	1.0	3.9	4.7	3.2	<u>2.1</u>	1.1
0.10	4.25	4.0	3.3	<u>2.35</u>	1.1	4.0	4.6	3.2	<u>2.2</u>	1.0	3.8	4.8	3.1	<u>2.3</u>	1.0
0.05	3.85	4.0	3.45	<u>2.6</u>	1.1	3.8	4.7	2.9	<u>2.2</u>	1.4	3.9	4.7	3.1	<u>2.3</u>	1.0
0.00	<u>2.95</u>	3.95	3.35	3.35	1.4	3.0	3.9	3.3	<u>2.5</u>	2.3	<u>2.6</u>	4.1	3.5	2.8	2.0

TABLE II: FGSM average ranks for CI, IBS, and NegLL metrics across all datasets. Lower number is better.

ϵ	Concordance Index					Integrated Brier Score					Negative Log Likelihood				
	DRAFT	Noise	FGSM	PGD	SAWAR	DRAFT	Noise	FGSM	PGD	SAWAR	DRAFT	Noise	FGSM	PGD	SAWAR
1.00	<u>2.8</u>	3.4	3.5	3.6	1.7	<u>2.6</u>	4.3	3.8	3.3	1.0	3.1	4.5	3.4	<u>3.0</u>	1.0
0.90	<u>3.1</u>	3.3	3.5	3.4	1.7	<u>3.0</u>	4.3	3.6	3.1	1.0	3.1	4.5	3.5	<u>2.9</u>	1.0
0.80	<u>3.0</u>	3.3	3.5	3.7	1.5	<u>3.0</u>	4.5	3.5	<u>3.0</u>	1.0	3.0	4.6	3.5	<u>2.9</u>	1.0
0.70	<u>3.05</u>	3.3	3.6	3.65	1.4	<u>3.0</u>	4.5	3.5	<u>3.0</u>	1.0	3.1	4.5	3.5	<u>2.9</u>	1.0
0.60	<u>2.85</u>	3.55	3.55	3.75	1.3	<u>3.0</u>	4.5	3.5	<u>3.0</u>	1.0	3.0	4.7	3.5	<u>2.8</u>	1.0
0.50	<u>3.2</u>	3.9	3.35	3.45	1.1	3.2	4.4	3.5	<u>2.9</u>	1.0	3.0	4.7	3.5	<u>2.8</u>	1.0
0.40	3.25	3.95	<u>3.2</u>	3.5	1.1	3.3	4.8	3.2	<u>2.7</u>	1.0	3.1	4.7	3.4	<u>2.8</u>	1.0
0.30	<u>3.0</u>	3.05	3.95	3.6	1.4	3.5	4.7	3.3	<u>2.5</u>	1.0	3.3	4.9	3.2	<u>2.6</u>	1.0
0.20	<u>2.05</u>	2.95	4.2	3.8	2.0	3.7	4.7	3.4	<u>2.2</u>	1.0	3.4	4.9	3.4	<u>2.3</u>	1.0
0.10	<u>2.85</u>	3.4	3.4	3.35	2.0	3.3	4.5	3.0	<u>2.3</u>	1.9	3.5	4.5	3.2	<u>2.2</u>	1.6
0.05	3.05	4.15	3.4	<u>2.9</u>	1.5	<u>2.6</u>	4.4	3.0	<u>2.6</u>	2.4	3.3	4.4	3.0	<u>2.4</u>	1.9
0.00	<u>2.95</u>	3.95	3.35	3.35	1.4	3.0	3.9	3.3	<u>2.5</u>	2.3	<u>2.6</u>	4.1	3.5	2.8	2.0

TABLE III: Worst-Case average ranks for CI, IBS, and NegLL metrics across all datasets. Lower number is better.

input covariates:

$$\tilde{S}(t|\mathbf{x}) = e^{-\tilde{\lambda}_{\theta}t}. \quad (24)$$

For the exponential CPH distribution, as the failure rate increases with the ϵ -perturbation, the probability of survival decreases monotonically. We use CROWN-IBP for a tight approximation to the upper bound on the maximization term in equation Eq. (23). We evaluate the SA metrics for $\epsilon \in [0, 1]$, where $\epsilon = 0$ is no perturbation to input covariates, for the two perturbations methods to study how sensitive each adversarial training method is to covariate perturbation.

Note that when the activation functions are piecewise linear, an exact solution can also be obtained by solving a Mixed Integer Linear Program (MILP). However, solving the MILP is computationally prohibitive: even for $\epsilon = 0.1$ each MILP takes on average 9-10 seconds when tested on the Dialysis dataset, whereas CROWN-IBP takes milliseconds to calculate over all the data in the Dialysis dataset.

D. Results

Furthermore, we analyze how adversarial perturbations impact the characteristics of the population survival curves.

1) *Failure Rate Distribution*: Let us assume that the input covariates are random variables $\mathbf{x} \sim p(\mathbf{x})$. Then the failure rate becomes a random variable that occurs from the stochasticity of the input covariates $\lambda \sim \lambda_{\theta}(\mathbf{x})$. Moreover, we treat $S_{\theta}(t|\mathbf{x})$ as a stochastic process :

$$S_{\theta}(t) \sim e^{-\lambda t} \quad (25)$$

Furthermore, we compute statistical quantities such as expectation, lower 5th quantile $LB = Q_{05}(\lambda_{\theta}(\mathbf{x}))$, and upper 95th quantile $UB = Q_{95}(\lambda_{\theta}(\mathbf{x}))$.

Fig. 1 visualizes the credible interval and mean of the survival function stochastic process in Eq. (25). The 90% credible interval of the the stochastic process changes with respect to the strength of the adversarial regularization method (Fig. 1). We observe the trend that the credible interval slightly narrows down as the strength of the adversarial regularization method increases (Fig. 1). The variance of the failure rate decreasing leads to a more robust model against adversarial perturbations. For example, when $\text{Var}(\lambda_{\theta}(\mathbf{x})) = 0$, then there is a mode collapse such that $\lambda(\mathbf{x}_i) = \lambda \forall i$. This is the case for point-estimates of the parameter λ derived via maximum likelihood estimation. A point-estimate results in a population curve, but no instance-level survival curves. Therefore, by utilizing a weighted objective in Eq. (21), we trade-off individualized survival curves with vulnerability to adversarial perturbations and a population survival curve which is completely resilient to adversarial perturbations.

However, despite exhibiting significantly higher adversarial robustness, the credible interval usually remains relatively unchanged compared to the DRAFT method.

2) *Population Survival Curve*: The ϵ -perturbation magnitude determines the severity of the worst-case survival curve. We observe the trend that the stronger the adversarial regularization method, the “closer” the ϵ -worst-case population curve becomes to the unperturbed population survival curve for a given $\epsilon \in [0, 1]$ (Fig. 2). Moreover, we use the Kaplan Meier Curve (KMC), a commonly used frequentist approach for non-parametrically estimating the population survival curve using samples $\{t_i, e_i\}_{i=1}^N$, to visually evaluate model calibration. The close alignment between the population survival curve and the KMC shown in Fig. 2 demonstrates the strong calibration of

SAWAR model [19].

We calculate the average ranking of each adversarial regularization method across all datasets with respect to CI, IBS, NegLL in response to the FGSM and ϵ -worst-case perturbations (Tables II and III). We empirically showed that CROWN-IBP adversarial regularization leads to increased performance, consistently ranking the best across various ϵ -perturbation magnitudes. More detailed results, along with the exact metric values for each ϵ of the worst-case perturbation for each dataset are available in the code repository linked in the abstract.

VII. CONCLUSIONS

This paper introduces CROWN-IBP regularization for enhancing adversarial robustness in fully-parametric SA using NN models. We evaluated the SAWAR method on 10 time-to-event medical datasets, comparing it with standard adversarial regularization methods such as Gaussian noise, FGSM, and PGD, as well as the novel worst-case perturbation.

Our empirical results show that CROWN-IBP regularization consistently improves performance in SA across various metrics, including CI, IBS, and NegLL, for all ϵ -perturbation magnitudes from 0 to 1. Compared to conventional adversarial regularization techniques, SAWAR demonstrates superior resilience to input covariate perturbations, with relative improvements in CI and IBS ranging from 1% to 150% across all ϵ -perturbation magnitudes.

In summary, SAWAR significantly enhances predictive performance, adversarial robustness, and calibration. This approach effectively mitigates data uncertainty in SA and improves generalization across unseen datasets.

Future work will include the use of the Weibull CPH model to enable time varying hazard rates. This will require extending `auto_LIRPA` to handle the power operator for operations such as t^k , where k is a learnable parameter.

REFERENCES

- [1] D. Altman, B. De Stavola, S. Love, and K. Stepniwska, "Review of survival analyses published in cancer journals," *British journal of cancer*, vol. 72, no. 2, pp. 511–518, 1995.
- [2] D. R. Cox, "The regression analysis of binary sequences," *Journal of the Royal Statistical Society Series B: Statistical Methodology*, vol. 20, no. 2, pp. 215–232, 1958.
- [3] B. Cheng and M. Potter, "Bayesian Weapon System Reliability Modeling with Cox-Weibull Neural Network," in *2023 Annual Reliability and Maintainability Symposium (RAMS)*, 2023, pp. 1–6.
- [4] R. C. Deo, "Machine learning in medicine," *Circulation*, vol. 132, no. 20, pp. 1920–1930, 2015.
- [5] G. Handelman, H. Kok, R. Chandra, A. Razavi, M. Lee, and H. Asadi, "Editor: machine learning and the future of medicine," *Journal of internal medicine*, vol. 284, no. 6, pp. 603–619, 2018.
- [6] A. Qayyum, J. Qadir, M. Bilal, and A. Al-Fuqaha, "Secure and robust machine learning for healthcare: A survey," *IEEE Reviews in Biomedical Engineering*, vol. 14, pp. 156–180, 2020.
- [7] F. J. Rodríguez-Vera, Y. Marín, A. Sánchez, C. Borrachero, and E. Pujol, "Illegible handwriting in medical records," *J R Soc Med*, vol. 95, no. 11, pp. 545–546, Nov 2002.
- [8] J. Li, Y. Mao, and J. Zhang, "Maintenance and quality control of medical equipment based on information fusion technology," *Comput Intell Neurosci*, vol. 2022, p. 9333328, Oct 2022.
- [9] E. R. Lenz, *Measurement in nursing and health research*. Springer publishing company, 2010.
- [10] L. V. Utkin, V. S. Zaborovsky, M. S. Kovalev, A. V. Konstantinov, N. A. Politaeva, and A. A. Lukashin, "Uncertainty interpretation of the machine learning survival model predictions," *IEEE Access*, vol. 9, pp. 120 158–120 175, 2021.
- [11] D. G. Kleinbaum and M. Klein, *Survival analysis a self-learning text*. Springer, 1996.
- [12] A. Schwarzschild, M. Goldblum, A. Gupta, J. P. Dickerson, and T. Goldstein, "Just how toxic is data poisoning? a unified benchmark for backdoor and data poisoning attacks," in *International Conference on Machine Learning*. PMLR, 2021, pp. 9389–9398.
- [13] S. Wiegerebe, P. Kopper, R. Sonabend, B. Bischl, and A. Bender, "Deep Learning for Survival Analysis: A Review," 2023.
- [14] D. Faraggi and R. Simon, "A neural network model for survival data," *Statistics in Medicine*, vol. 14, no. 1, pp. 73–82, 1995. [Online]. Available: <https://onlinelibrary.wiley.com/doi/abs/10.1002/sim.4780140108>
- [15] T. Ching, X. Zhu, and L. X. Garmire, "Cox-nnet: An artificial neural network method for prognosis prediction of high-throughput omics data," *PLOS Computational Biology*, vol. 14, no. 4, pp. 1–18, 04 2018. [Online]. Available: <https://doi.org/10.1371/journal.pcbi.1006076>
- [16] J. L. Katzman, U. Shaham, A. Cloninger, J. Bates, T. Jiang, and Y. Kluger, "Deepsurv: personalized treatment recommender system using a cox proportional hazards deep neural network," *BMC Medical Research Methodology*, vol. 18, no. 1, p. 24, Feb 26 2018. [Online]. Available: <https://doi.org/10.1186/s12874-018-0482-1>
- [17] A. Bennis, S. Mouysset, and M. Serrurier, "Estimation of conditional mixture weibull distribution with right censored data using neural network for time-to-event analysis," in *Advances in Knowledge Discovery and Data Mining: 24th Pacific-Asia Conference, PAKDD 2020, Singapore, May 11–14, 2020, Proceedings, Part I 24*. Springer, 2020, pp. 687–698.
- [18] H. Haider, B. Hoehn, S. Davis, and R. Greiner, "Effective ways to build and evaluate individual survival distributions," *The Journal of Machine Learning Research*, vol. 21, no. 1, pp. 3289–3351, 2020.
- [19] M. Goldstein, X. Han, A. Puli, A. Perotte, and R. Ranganath, "X-cal: Explicit calibration for survival analysis," *Advances in neural information processing systems*, vol. 33, pp. 18 296–18 307, 2020.
- [20] F. Kamran and J. Wiens, "Estimating calibrated individualized survival curves with deep learning," in *Proceedings of the AAAI Conference on Artificial Intelligence*, vol. 35, no. 1, 2021, pp. 240–248.
- [21] C. Guo, G. Pleiss, Y. Sun, and K. Q. Weinberger, "On calibration of modern neural networks," in *International conference on machine learning*. PMLR, 2017, pp. 1321–1330.
- [22] I. J. Goodfellow, J. Shlens, and C. Szegedy, "Explaining and harnessing adversarial examples," *arXiv preprint arXiv:1412.6572*, 2014.
- [23] R. Vasilev and A. D'yakonov, "Calibration of neural networks," 2023.
- [24] Y. Qin, X. Wang, A. Beutel, and E. Chi, "Improving calibration through the relationship with adversarial robustness," *Advances in Neural Information Processing Systems*, vol. 34, pp. 14 358–14 369, 2021.
- [25] P. Chapfuwa, C. Tao, C. Li, C. Page, B. Goldstein, L. C. Duke, and R. Henao, "Adversarial time-to-event modeling," in *Proceedings of the 35th International Conference on Machine Learning*, ser. Proceedings of Machine Learning Research, J. Dy and A. Krause, Eds., vol. 80. PMLR, 10–15 Jul 2018, pp. 735–744. [Online]. Available: <https://proceedings.mlr.press/v80/chapfuwa18a.html>
- [26] T. Uemura, J. J. Näppi, C. Watari, T. Hironaka, T. Kamiya, and H. Yoshida, "Weakly unsupervised conditional generative adversarial network for image-based prognostic prediction for covid-19 patients based on chest ct," *Medical Image Analysis*, vol. 73, p. 102159, 2021. [Online]. Available: <https://www.sciencedirect.com/science/article/pii/S136184152100205X>
- [27] P. Liu, L. Ji, F. Ye, and B. Fu, "Advmil: Adversarial multiple instance learning for the survival analysis on whole-slide images," *Medical Image Analysis*, vol. 91, p. 103020, 2024. [Online]. Available: <https://www.sciencedirect.com/science/article/pii/S1361841523002803>
- [28] C. M. Bishop and N. M. Nasrabadi, *Pattern recognition and machine learning*. Springer, 2006, vol. 4, no. 4.
- [29] I. Goodfellow, "Nips 2016 tutorial: Generative adversarial networks," 2017.
- [30] K. P. Murphy, *Machine learning: a probabilistic perspective*. MIT press, 2012.
- [31] R. Bender, T. Augustin, and M. Blettner, "Generating survival times to simulate cox proportional hazards models," *Statistics in medicine*, vol. 24, no. 11, pp. 1713–1723, 2005.

- [32] C. Stanley, E. Molyneux, and M. Mukaka, "Comparison of performance of exponential, cox proportional hazards, weibull and frailty survival models for analysis of small sample size data," *Journal of Medical Statistics and Informatics*, vol. 4, no. 1, 2016.
- [33] P. Royston, "Flexible parametric alternatives to the cox model, and more," *The Stata Journal*, vol. 1, no. 1, pp. 1–28, 2001.
- [34] L. Kleinrock, *Theory, Volume 1, Queueing Systems*. USA: Wiley-Interscience, 1975.
- [35] R. B. Cooper, "Queueing theory," in *Proceedings of the ACM'81 conference*, 1981, pp. 119–122.
- [36] S. P. Jenkins, "Survival analysis," *Unpublished manuscript, Institute for Social and Economic Research, University of Essex, Colchester, UK*, vol. 42, pp. 54–56, 2005.
- [37] G. Rodriguez, "Parametric survival models," *Rapport technique, Princeton: Princeton University*, 2010.
- [38] C. Lee, J. Yoon, and M. Van Der Schaar, "Dynamic-deephit: A deep learning approach for dynamic survival analysis with competing risks based on longitudinal data," *IEEE Transactions on Biomedical Engineering*, vol. 67, no. 1, pp. 122–133, 2019.
- [39] S. Pölsterl, "scikit-survival: A Library for Time-to-Event Analysis Built on Top of scikit-learn," *Journal of Machine Learning Research*, vol. 21, no. 212, pp. 1–6, 2020. [Online]. Available: <http://jmlr.org/papers/v21/20-729.html>
- [40] A. D. Palma, R. Bunel, K. Dvijotham, M. P. Kumar, and R. Stanforth, "IBP Regularization for Verified Adversarial Robustness via Branch-and-Bound," 2023.
- [41] H. Zhang, H. Chen, C. Xiao, S. Goyal, R. Stanforth, B. Li, D. Boning, and C.-J. Hsieh, "Towards stable and efficient training of verifiably robust neural networks," 2019.
- [42] A. Madry, A. Makelov, L. Schmidt, D. Tsipras, and A. Vladu, "Towards Deep Learning Models Resistant to Adversarial Attacks," 2019.
- [43] S. Goyal, K. Dvijotham, R. Stanforth, R. Bunel, C. Qin, J. Uesato, R. Arandjelovic, T. A. Mann, and P. Kohli, "On the Effectiveness of Interval Bound Propagation for Training Verifiably Robust Models," *CoRR*, vol. abs/1810.12715, 2018. [Online]. Available: <http://arxiv.org/abs/1810.12715>
- [44] K. Xu, Z. Shi, H. Zhang, Y. Wang, K.-W. Chang, M. Huang, B. Kailkhura, X. Lin, and C.-J. Hsieh, "Automatic Perturbation Analysis for Scalable Certified Robustness and Beyond," 2020.
- [45] I. J. Goodfellow, J. Shlens, and C. Szegedy, "Explaining and harnessing adversarial examples," *arXiv preprint arXiv:1412.6572*, 2014.
- [46] E. Rusak, L. Schott, R. S. Zimmermann, J. Bitterwolf, O. Bringmann, M. Bethge, and W. Brendel, "A simple way to make neural networks robust against diverse image corruptions," in *Computer Vision—ECCV 2020: 16th European Conference, Glasgow, UK, August 23–28, 2020, Proceedings, Part III 16*. Springer, 2020, pp. 53–69.
- [47] D. P. Kingma and J. Ba, "Adam: A method for stochastic optimization," 2017.
- [48] Y. Yao, L. Rosasco, and A. Caponnetto, "On Early Stopping in Gradient Descent Learning," *Constructive Approximation*, vol. 26, no. 2, pp. 289–315, August 1 2007. [Online]. Available: <https://doi.org/10.1007/s00365-006-0663-2>
- [49] J. Harrell, Frank E., R. M. Califf, D. B. Pryor, K. L. Lee, and R. A. Rosati, "Evaluating the Yield of Medical Tests," *JAMA*, vol. 247, no. 18, pp. 2543–2546, 05 1982. [Online]. Available: <https://doi.org/10.1001/jama.1982.03320430047030>
- [50] E. Graf, C. Schmoor, W. Sauerbrei, and M. Schumacher, "Assessment and comparison of prognostic classification schemes for survival data," *Statistics in Medicine*, vol. 18, no. 17–18, pp. 2529–2545, 1999.
- [51] C. Davidson-Pilon, "lifelines: survival analysis in python," *Journal of Open Source Software*, vol. 4, no. 40, p. 1317, 2019. [Online]. Available: <https://doi.org/10.21105/joss.01317>
- [52] E. Drysdale, "SurvSet: An open-source time-to-event dataset repository," 2022.
- [53] G. V. H. Jensen, C. Torp-Pedersen, P. Hildebrandt, L. Kober, F. Nielsen, T. Melchior, T. Joen, and P. Andersen, "Does in-hospital ventricular fibrillation affect prognosis after myocardial infarction?" *European heart journal*, vol. 18, no. 6, pp. 919–924, 1997.
- [54] "Stage C Prostate Cancer," <https://rdrr.io/cran/rpart/man/stagec.html>.
- [55] R. A. Kyle, T. M. Therneau, S. V. Rajkumar, D. R. Larson, M. F. Plevak, J. R. Offord, A. Dispenzieri, J. A. Katzmann, and L. J. Melton III, "Prevalence of monoclonal gammopathy of undetermined significance," *New England Journal of Medicine*, vol. 354, no. 13, pp. 1362–1369, 2006.
- [56] B. D. Ripley, *Modern applied statistics with S*. springer, 2002.
- [57] T. J. Wang, J. M. Massaro, D. Levy, R. S. Vasan, P. A. Wolf, R. B. D'Agostino, M. G. Larson, W. B. Kannel, and E. J. Benjamin, "A risk score for predicting stroke or death in individuals with new-onset atrial fibrillation in the community: the framingham heart study," *Jama*, vol. 290, no. 8, pp. 1049–1056, 2003.
- [58] "dataDIVAT1," <https://rdrr.io/cran/RISCA/man/dataDIVAT1.html>.
- [59] "Prostate dataset," <https://hbiostat.org/data/repo/cprostate>.
- [60] C. C. Abnet, B. Lai, Y.-L. Qiao, S. Vogt, X.-M. Luo, P. R. Taylor, Z.-W. Dong, S. D. Mark, and S. M. Dawsey, "Zinc concentration in esophageal biopsy specimens measured by x-ray fluorescence and esophageal cancer risk," *Journal of the National Cancer Institute*, vol. 97, no. 4, pp. 301–306, 2005.
- [61] A. Blair, D. Hadden, J. Weaver, D. Archer, P. Johnston, and C. Maguire, "The 5-year prognosis for vision in diabetes." *The Ulster medical journal*, vol. 49, no. 2, p. 139, 1980.
- [62] R. Henderson, S. Shimakura, and D. Gorst, "Modeling spatial variation in leukemia survival data," *Journal of the American Statistical Association*, vol. 97, no. 460, pp. 965–972, 2002.

APPENDIX

We find that as the ϵ -perturbation magnitude increases from 0 to 1, the relative percentage change from DRAFT to the adversarial training methods becomes larger and then smaller. The relative percent changes in CI from the DRAFT training objective to SAWAR training objective is shown in Table IV (where higher percentage change is better). We note that for very large ϵ , since our data is standard normalized all methods begin to fail.

ϵ	1.00	0.90	0.80	0.70	0.60	0.50	0.40	0.30	0.20	0.10	0.05	0.00
$\% \Delta$	29.46	48.18	56.27	72.23	102.44	133.35	152.17	140.33	91.78	21.17	9.63	1.07

TABLE IV: The relative percent change in Concordance Index metric from the DRAFT training objective to the SAWAR training objective averaged across the *SurvSet* datasets. A higher relative percent change is better.

	ϵ	1.00	0.90	0.80	0.70	0.60	0.50	0.40	0.30	0.20	0.10	0.05	0.00
Aids2	DRAFT	0.499	0.497	0.501	0.505	0.507	0.509	0.517	0.535	0.565	0.573	0.573	0.572
	Noise	0.492	0.494	0.496	0.5	0.5	0.498	0.507	0.526	0.556	0.556	0.554	0.554
	FGSM	0.498	0.495	0.498	0.497	0.5	0.502	0.508	0.529	0.554	0.557	0.555	0.553
	PGD	0.498	0.497	0.497	0.5	0.501	0.501	0.507	0.531	0.557	0.558	0.556	0.554
	SAWAR	0.567	0.575	0.577	0.579	0.58	0.58	0.579	0.579	0.579	0.579	0.579	0.579
Framingham	DRAFT	0.612	0.623	0.635	0.646	0.656	0.664	0.672	0.678	0.682	0.686	0.687	0.688
	Noise	0.606	0.616	0.626	0.635	0.642	0.649	0.659	0.674	0.683	0.685	0.685	0.685
	FGSM	0.607	0.611	0.617	0.622	0.626	0.635	0.652	0.669	0.682	0.686	0.687	0.686
	PGD	0.567	0.578	0.588	0.599	0.61	0.624	0.642	0.659	0.68	0.688	0.688	0.687
	SAWAR	0.694	0.697	0.699	0.701	0.702	0.704	0.704	0.705	0.705	0.704	0.704	0.704
LeukSurv	DRAFT	0.611	0.616	0.623	0.623	0.627	0.631	0.63	0.631	0.63	0.624	0.624	0.626
	Noise	0.552	0.557	0.562	0.566	0.569	0.574	0.587	0.61	0.628	0.627	0.621	0.617
	FGSM	0.546	0.549	0.554	0.563	0.561	0.566	0.583	0.602	0.624	0.624	0.621	0.62
	PGD	0.537	0.536	0.538	0.549	0.546	0.558	0.577	0.598	0.62	0.622	0.619	0.617
	SAWAR	0.483	0.498	0.51	0.532	0.553	0.583	0.589	0.607	0.617	0.623	0.632	0.636
TRACE	DRAFT	0.564	0.586	0.612	0.637	0.665	0.69	0.714	0.73	0.734	0.733	0.735	0.735
	Noise	0.565	0.588	0.613	0.64	0.668	0.692	0.716	0.73	0.733	0.735	0.734	0.735
	FGSM	0.553	0.577	0.603	0.63	0.658	0.688	0.713	0.722	0.727	0.73	0.733	0.734
	PGD	0.557	0.582	0.609	0.636	0.664	0.696	0.723	0.731	0.733	0.732	0.733	0.733
	SAWAR	0.73	0.733	0.736	0.738	0.739	0.739	0.74	0.74	0.739	0.738	0.738	0.737
dataDIVAT1	DRAFT	0.534	0.558	0.583	0.606	0.624	0.639	0.65	0.658	0.662	0.664	0.664	0.664
	Noise	0.534	0.539	0.551	0.571	0.587	0.612	0.636	0.656	0.654	0.64	0.635	0.631
	FGSM	0.575	0.585	0.594	0.606	0.617	0.628	0.638	0.644	0.651	0.643	0.638	0.635
	PGD	0.517	0.529	0.548	0.568	0.591	0.618	0.636	0.654	0.657	0.651	0.647	0.644
	SAWAR	0.627	0.642	0.652	0.658	0.659	0.659	0.659	0.658	0.657	0.656	0.656	0.655
fchain	DRAFT	0.096	0.098	0.102	0.107	0.114	0.127	0.156	0.461	0.9	0.916	0.922	0.924
	Noise	0.096	0.099	0.104	0.112	0.127	0.164	0.335	0.768	0.912	0.921	0.923	0.923
	FGSM	0.102	0.116	0.159	0.288	0.599	0.852	0.91	0.917	0.923	0.927	0.927	0.925
	PGD	0.102	0.127	0.235	0.538	0.824	0.904	0.917	0.921	0.925	0.929	0.929	0.929
	SAWAR	0.84	0.925	0.927	0.929	0.93	0.93	0.929	0.929	0.93	0.93	0.931	0.931
prostate	DRAFT	0.412	0.419	0.426	0.447	0.463	0.49	0.53	0.581	0.614	0.635	0.639	0.643
	Noise	0.49	0.503	0.514	0.524	0.533	0.541	0.553	0.566	0.576	0.572	0.577	0.576
	FGSM	0.514	0.522	0.526	0.536	0.541	0.549	0.558	0.573	0.582	0.596	0.596	0.596
	PGD	0.522	0.526	0.532	0.535	0.54	0.548	0.557	0.567	0.576	0.593	0.591	0.593
	SAWAR	0.575	0.584	0.598	0.6	0.608	0.632	0.638	0.638	0.639	0.641	0.642	0.644
retinopathy	DRAFT	0.525	0.539	0.562	0.569	0.587	0.592	0.592	0.599	0.605	0.601	0.604	0.605
	Noise	0.526	0.545	0.561	0.57	0.581	0.588	0.588	0.6	0.603	0.6	0.604	0.606
	FGSM	0.47	0.485	0.51	0.536	0.569	0.578	0.591	0.6	0.599	0.602	0.606	0.607
	PGD	0.471	0.481	0.509	0.53	0.567	0.577	0.591	0.599	0.598	0.601	0.606	0.607
	SAWAR	0.588	0.597	0.611	0.616	0.619	0.615	0.621	0.62	0.62	0.619	0.617	0.617
stagec	DRAFT	0.442	0.457	0.476	0.495	0.514	0.548	0.582	0.668	0.721	0.697	0.688	0.688
	Noise	0.471	0.481	0.505	0.49	0.514	0.534	0.582	0.697	0.721	0.712	0.688	0.697
	FGSM	0.423	0.438	0.447	0.471	0.51	0.567	0.62	0.663	0.688	0.678	0.688	0.688
	PGD	0.462	0.486	0.471	0.495	0.51	0.567	0.611	0.668	0.692	0.688	0.697	0.697
	SAWAR	0.428	0.447	0.481	0.514	0.567	0.639	0.673	0.692	0.702	0.692	0.692	0.707
zinc	DRAFT	0.339	0.349	0.356	0.376	0.427	0.507	0.657	0.758	0.796	0.796	0.792	0.793
	Noise	0.315	0.329	0.339	0.376	0.424	0.545	0.704	0.778	0.791	0.805	0.806	0.81
	FGSM	0.339	0.357	0.384	0.439	0.55	0.657	0.738	0.776	0.787	0.804	0.809	0.812
	PGD	0.333	0.351	0.384	0.439	0.55	0.671	0.738	0.776	0.79	0.8	0.809	0.808
	SAWAR	0.383	0.464	0.533	0.649	0.707	0.746	0.766	0.779	0.789	0.787	0.795	0.8

TABLE V: Concordance Index metric for *SurvSet* datasets (higher is better) for each adversarial training method against the worst-case adversarial attack.

We find that as the ϵ -perturbation magnitude increases from 0 to 1, the relative percentage change from DRAFT to the adversarial training methods becomes larger and then smaller. The relative percent changes in Integrated Brier Score metric from the DRAFT training objective to SAWAR training objective is shown in Table VI (where lower percentage change is better). We note that for very large ϵ , since our data is standard normalized all methods begin to fail.

ϵ	1.00	0.90	0.80	0.70	0.60	0.50	0.40	0.30	0.20	0.10	0.05	0.00
% Δ	-44.13	-45.46	-46.68	-47.57	-47.86	-47.10	-45.03	-40.89	-33.06	-20.29	-11.34	-1.68

TABLE VI: The relative percent change in Integrated Brier Score metric from the DRAFT training objective to the SAWAR training objective averaged across the *SurvSet* datasets. A lower relative percent change is better.

	ϵ	1.00	0.90	0.80	0.70	0.60	0.50	0.40	0.30	0.20	0.10	0.05	0.00
Aids2	DRAFT	0.24	0.233	0.224	0.212	0.197	0.178	0.157	0.137	0.124	0.12	0.121	0.122
	Noise	0.254	0.253	0.25	0.245	0.236	0.22	0.196	0.161	0.13	0.121	0.121	0.122
	FGSM	0.252	0.249	0.244	0.236	0.223	0.203	0.176	0.145	0.125	0.121	0.121	0.121
	PGD	0.252	0.248	0.243	0.234	0.221	0.2	0.172	0.143	0.124	0.121	0.121	0.121
	SAWAR	0.126	0.124	0.124	0.124	0.123	0.123	0.123	0.123	0.123	0.123	0.123	0.124
Framingham	DRAFT	0.81	0.8	0.778	0.733	0.65	0.52	0.369	0.243	0.165	0.128	0.119	0.115
	Noise	0.818	0.818	0.816	0.809	0.778	0.681	0.495	0.294	0.174	0.128	0.119	0.116
	FGSM	0.818	0.816	0.81	0.791	0.728	0.58	0.369	0.208	0.14	0.12	0.116	0.115
	PGD	0.818	0.818	0.817	0.811	0.784	0.683	0.461	0.235	0.138	0.117	0.115	0.115
	SAWAR	0.165	0.152	0.141	0.133	0.127	0.122	0.118	0.116	0.114	0.114	0.113	0.113
LeukSurv	DRAFT	0.163	0.163	0.163	0.163	0.162	0.161	0.156	0.144	0.126	0.109	0.105	0.103
	Noise	0.163	0.163	0.163	0.163	0.163	0.163	0.163	0.163	0.157	0.134	0.12	0.114
	FGSM	0.163	0.163	0.163	0.163	0.163	0.163	0.161	0.148	0.122	0.114	0.111	0.111
	PGD	0.163	0.163	0.163	0.163	0.163	0.163	0.163	0.16	0.145	0.12	0.114	0.111
	SAWAR	0.154	0.15	0.144	0.136	0.128	0.12	0.115	0.112	0.11	0.107	0.107	0.106
TRACE	DRAFT	0.634	0.634	0.633	0.626	0.603	0.549	0.449	0.329	0.234	0.183	0.172	0.167
	Noise	0.634	0.634	0.632	0.622	0.596	0.536	0.435	0.319	0.23	0.183	0.172	0.167
	FGSM	0.634	0.634	0.634	0.631	0.613	0.555	0.434	0.294	0.212	0.177	0.171	0.168
	PGD	0.634	0.634	0.632	0.621	0.58	0.491	0.362	0.245	0.189	0.171	0.167	0.166
	SAWAR	0.282	0.254	0.231	0.213	0.198	0.186	0.177	0.17	0.166	0.163	0.163	0.163
dataDIVAT1	DRAFT	0.721	0.702	0.67	0.616	0.531	0.417	0.308	0.234	0.195	0.18	0.178	0.178
	Noise	0.749	0.749	0.748	0.748	0.743	0.72	0.626	0.413	0.248	0.198	0.192	0.192
	FGSM	0.749	0.749	0.748	0.747	0.74	0.699	0.547	0.322	0.215	0.193	0.192	0.192
	PGD	0.749	0.749	0.749	0.748	0.746	0.724	0.582	0.305	0.192	0.184	0.186	0.187
	SAWAR	0.266	0.241	0.224	0.212	0.202	0.193	0.187	0.183	0.18	0.178	0.178	0.178
f1chaim	DRAFT	0.831	0.831	0.831	0.831	0.831	0.83	0.829	0.818	0.486	0.096	0.07	0.052
	Noise	0.831	0.831	0.831	0.831	0.831	0.83	0.829	0.807	0.25	0.087	0.063	0.052
	FGSM	0.831	0.831	0.831	0.83	0.83	0.828	0.707	0.146	0.094	0.06	0.054	0.051
	PGD	0.831	0.831	0.831	0.83	0.83	0.797	0.298	0.114	0.079	0.055	0.051	0.05
	SAWAR	0.522	0.161	0.076	0.063	0.057	0.054	0.052	0.051	0.05	0.05	0.049	0.049
prostate	DRAFT	0.53	0.529	0.528	0.526	0.519	0.505	0.475	0.418	0.335	0.256	0.231	0.218
	Noise	0.53	0.53	0.53	0.53	0.53	0.53	0.53	0.528	0.477	0.371	0.325	0.296
	FGSM	0.53	0.53	0.53	0.53	0.53	0.53	0.529	0.509	0.413	0.29	0.257	0.246
	PGD	0.53	0.53	0.53	0.53	0.53	0.53	0.528	0.502	0.396	0.28	0.254	0.244
	SAWAR	0.508	0.482	0.441	0.393	0.348	0.309	0.278	0.251	0.229	0.214	0.209	0.205
retinopathy	DRAFT	0.662	0.657	0.645	0.621	0.582	0.522	0.43	0.324	0.244	0.203	0.196	0.195
	Noise	0.662	0.657	0.645	0.622	0.583	0.523	0.432	0.326	0.245	0.204	0.196	0.195
	FGSM	0.656	0.646	0.626	0.597	0.556	0.493	0.401	0.301	0.232	0.201	0.196	0.197
	PGD	0.656	0.645	0.625	0.596	0.554	0.49	0.397	0.299	0.231	0.201	0.197	0.198
	SAWAR	0.526	0.484	0.436	0.385	0.334	0.29	0.254	0.228	0.211	0.203	0.202	0.202
stagec	DRAFT	0.505	0.505	0.505	0.504	0.502	0.486	0.431	0.329	0.211	0.175	0.181	0.192
	Noise	0.505	0.505	0.505	0.504	0.502	0.485	0.432	0.338	0.216	0.175	0.181	0.192
	FGSM	0.505	0.505	0.505	0.503	0.494	0.458	0.382	0.268	0.174	0.161	0.169	0.178
	PGD	0.505	0.505	0.505	0.503	0.493	0.454	0.377	0.261	0.169	0.159	0.167	0.176
	SAWAR	0.491	0.476	0.45	0.408	0.354	0.296	0.24	0.195	0.168	0.16	0.162	0.167
zinc	DRAFT	0.907	0.907	0.905	0.899	0.882	0.823	0.652	0.368	0.18	0.109	0.096	0.09
	Noise	0.908	0.907	0.907	0.904	0.893	0.838	0.625	0.32	0.168	0.109	0.096	0.089
	FGSM	0.907	0.907	0.904	0.892	0.839	0.659	0.365	0.194	0.124	0.095	0.089	0.086
	PGD	0.907	0.907	0.903	0.89	0.832	0.64	0.348	0.187	0.122	0.094	0.088	0.087
	SAWAR	0.72	0.609	0.476	0.352	0.26	0.198	0.159	0.132	0.113	0.1	0.096	0.094

TABLE VII: Integrated Brier Score metric for *SurvSet* datasets (lower is better) for each adversarial training method against the worst-case adversarial attack.

	ϵ	1.00	0.90	0.80	0.70	0.60	0.50	0.40	0.30	0.20	0.10	0.05	0.00
Aids2	DRAFT	1.14e+04	7.22e+03	4.60e+03	2.87e+03	1.80e+03	1.16e+03	7.95e+02	6.06e+02	5.32e+02	5.16e+02	5.17e+02	5.19e+02
	Noise	3.84e+05	1.61e+05	6.68e+04	2.78e+04	1.14e+04	4.42e+03	1.83e+03	8.54e+02	5.64e+02	5.20e+02	5.19e+02	5.21e+02
	FGSM	6.77e+04	3.50e+04	1.78e+04	8.89e+03	4.35e+03	2.14e+03	1.10e+03	6.66e+02	5.35e+02	5.19e+02	5.19e+02	5.20e+02
	PGD	5.49e+04	2.86e+04	1.49e+04	7.58e+03	3.79e+03	1.92e+03	1.02e+03	6.42e+02	5.31e+02	5.19e+02	5.19e+02	5.19e+02
	SAWAR	5.29e+02	5.24e+02	5.22e+02	5.22e+02	5.21e+02	5.21e+02	5.21e+02	5.21e+02	5.21e+02	5.22e+02	5.22e+02	5.22e+02
Framingham	DRAFT	1.47e+05	7.07e+04	3.42e+04	1.68e+04	8.47e+03	4.57e+03	2.79e+03	2.01e+03	1.68e+03	1.54e+03	1.51e+03	1.50e+03
	Noise	1.27e+07	3.17e+06	8.03e+05	2.06e+05	5.38e+04	1.48e+04	4.92e+03	2.39e+03	1.72e+03	1.54e+03	1.51e+03	1.50e+03
	FGSM	1.95e+06	5.96e+05	1.84e+05	5.70e+04	1.81e+04	6.33e+03	2.84e+03	1.85e+03	1.58e+03	1.51e+03	1.50e+03	1.49e+03
	PGD	2.01e+07	4.36e+06	9.57e+05	2.13e+05	4.88e+04	1.21e+04	3.85e+03	1.97e+03	1.57e+03	1.50e+03	1.49e+03	1.49e+03
	SAWAR	1.66e+03	1.62e+03	1.58e+03	1.56e+03	1.53e+03	1.52e+03	1.50e+03	1.50e+03	1.49e+03	1.49e+03	1.49e+03	1.49e+03
LeukSurv	DRAFT	1.79e+07	4.80e+06	1.29e+06	3.48e+05	9.29e+04	2.53e+04	6.59e+03	1.77e+03	5.76e+02	3.10e+02	2.74e+02	2.58e+02
	Noise	5.46e+23	1.79e+21	7.98e+18	2.52e+16	8.53e+13	1.88e+11	5.25e+08	2.35e+06	3.37e+04	2.60e+03	1.21e+03	7.21e+02
	FGSM	8.34e+16	1.79e+15	3.10e+13	4.86e+11	8.13e+09	1.49e+08	2.72e+06	7.03e+04	3.45e+03	6.20e+02	4.31e+02	3.59e+02
	PGD	1.28e+15	3.89e+13	1.03e+12	2.67e+10	7.96e+08	2.30e+07	7.01e+05	2.80e+04	1.98e+03	4.65e+02	3.58e+02	3.17e+02
	SAWAR	2.07e+04	8.38e+03	3.50e+03	1.45e+03	6.62e+02	3.45e+02	2.91e+02	2.70e+02	2.60e+02	2.54e+02	2.52e+02	2.50e+02
TRACE	DRAFT	4.56e+09	4.41e+08	4.44e+07	4.61e+06	5.31e+05	6.71e+04	9.88e+03	2.20e+03	9.05e+02	6.03e+02	5.53e+02	5.32e+02
	Noise	9.11e+08	1.07e+08	1.34e+07	1.74e+06	2.43e+05	3.71e+04	6.63e+03	1.78e+03	8.35e+02	5.93e+02	5.51e+02	5.32e+02
	FGSM	2.01e+11	9.10e+09	4.31e+08	2.24e+07	1.26e+06	8.26e+04	7.79e+03	1.61e+03	7.45e+02	5.74e+02	5.47e+02	5.35e+02
	PGD	4.53e+08	4.81e+07	5.35e+06	6.12e+05	7.63e+04	1.07e+04	2.09e+03	8.37e+02	5.94e+02	5.40e+02	5.31e+02	5.26e+02
	SAWAR	8.79e+02	7.60e+02	6.82e+02	6.29e+02	5.94e+02	5.69e+02	5.53e+02	5.41e+02	5.33e+02	5.28e+02	5.27e+02	5.27e+02
dataDIVAT1	DRAFT	1.43e+04	8.36e+03	4.95e+03	3.01e+03	1.91e+03	1.31e+03	9.99e+02	8.51e+02	7.84e+02	7.56e+02	7.51e+02	7.49e+02
	Noise	5.69e+08	7.64e+07	1.05e+07	1.44e+06	2.07e+05	3.17e+04	5.75e+03	1.61e+03	9.08e+02	7.81e+02	7.67e+02	7.64e+02
	FGSM	2.48e+08	3.36e+07	4.65e+06	6.56e+05	9.64e+04	1.54e+04	3.12e+03	1.14e+03	8.16e+02	7.65e+02	7.61e+02	7.60e+02
	PGD	1.85e+11	8.02e+09	3.47e+08	1.75e+07	9.39e+05	6.14e+04	5.80e+03	1.27e+03	8.03e+02	7.57e+02	7.56e+02	7.57e+02
	SAWAR	9.18e+02	8.55e+02	8.21e+02	8.00e+02	7.86e+02	7.75e+02	7.66e+02	7.59e+02	7.55e+02	7.52e+02	7.51e+02	7.51e+02
flchain	DRAFT	3.35e+23	9.34e+20	2.56e+18	7.37e+15	2.23e+13	6.82e+10	2.29e+08	9.33e+05	1.67e+04	2.03e+03	1.25e+03	1.09e+03
	Noise	2.18e+35	1.20e+31	7.58e+26	4.68e+22	3.48e+18	2.65e+14	2.21e+10	6.77e+06	4.45e+04	1.96e+03	1.22e+03	1.11e+03
	FGSM	1.61e+20	3.47e+17	7.79e+14	1.86e+12	5.49e+09	4.02e+07	6.37e+05	1.86e+04	2.15e+03	1.15e+03	1.09e+03	1.08e+03
	PGD	1.30e+16	7.91e+13	4.93e+11	3.47e+09	4.60e+07	1.33e+06	4.93e+04	4.99e+03	1.45e+03	1.10e+03	1.08e+03	1.07e+03
	SAWAR	6.31e+03	2.22e+03	1.43e+03	1.19e+03	1.12e+03	1.09e+03	1.08e+03	1.07e+03	1.07e+03	1.07e+03	1.07e+03	1.07e+03
prostate	DRAFT	9.74e+05	3.22e+05	1.06e+05	3.58e+04	1.21e+04	4.25e+03	1.64e+03	7.62e+02	4.66e+02	3.70e+02	3.51e+02	3.44e+02
	Noise	7.00e+20	5.05e+18	3.75e+16	2.85e+14	2.28e+12	2.03e+10	2.59e+08	9.04e+06	4.85e+05	6.66e+04	2.94e+04	1.37e+04
	FGSM	3.16e+14	1.04e+13	3.40e+11	1.16e+10	4.07e+08	1.52e+07	6.47e+05	3.56e+04	3.75e+03	1.03e+03	7.20e+02	5.82e+02
	PGD	8.84e+12	4.29e+11	2.18e+10	1.14e+09	5.94e+07	3.27e+06	1.92e+05	1.44e+04	1.91e+03	6.40e+02	5.00e+02	4.39e+02
	SAWAR	9.65e+03	3.88e+03	1.66e+03	8.48e+02	5.43e+02	4.30e+02	3.83e+02	3.59e+02	3.45e+02	3.37e+02	3.35e+02	3.34e+02
retinopathy	DRAFT	1.11e+04	5.64e+03	2.88e+03	1.51e+03	8.08e+02	4.64e+02	2.98e+02	2.18e+02	1.84e+02	1.70e+02	1.68e+02	1.67e+02
	Noise	1.11e+04	5.61e+03	2.88e+03	1.51e+03	8.13e+02	4.68e+02	2.99e+02	2.19e+02	1.84e+02	1.70e+02	1.68e+02	1.68e+02
	FGSM	7.43e+03	3.89e+03	2.07e+03	1.12e+03	6.33e+02	3.86e+02	2.63e+02	2.03e+02	1.78e+02	1.68e+02	1.67e+02	1.68e+02
	PGD	7.30e+03	3.83e+03	2.04e+03	1.11e+03	6.25e+02	3.81e+02	2.60e+02	2.02e+02	1.77e+02	1.68e+02	1.67e+02	1.68e+02
	SAWAR	4.02e+02	3.31e+02	2.79e+02	2.41e+02	2.14e+02	1.95e+02	1.82e+02	1.74e+02	1.69e+02	1.67e+02	1.67e+02	1.67e+02
stagec	DRAFT	1.16e+06	2.94e+05	7.50e+04	1.85e+04	4.81e+03	1.28e+03	3.57e+02	1.14e+02	5.35e+01	4.10e+01	3.98e+01	3.97e+01
	Noise	2.07e+06	4.93e+05	1.14e+05	2.73e+04	6.49e+03	1.61e+03	4.19e+02	1.25e+02	5.50e+01	4.10e+01	3.96e+01	3.95e+01
	FGSM	1.80e+05	5.45e+04	1.67e+04	5.23e+03	1.64e+03	5.30e+02	1.77e+02	7.43e+01	4.54e+01	3.96e+01	3.91e+01	3.92e+01
	PGD	1.54e+05	4.77e+04	1.47e+04	4.63e+03	1.47e+03	4.84e+02	1.69e+02	7.23e+01	4.48e+01	3.93e+01	3.89e+01	3.90e+01
	SAWAR	1.03e+03	5.79e+02	3.30e+02	1.94e+02	1.21e+02	8.21e+01	6.10e+01	4.88e+01	4.22e+01	3.89e+01	3.83e+01	3.81e+01
zinc	DRAFT	2.62e+06	5.85e+05	1.33e+05	3.13e+04	7.43e+03	1.87e+03	5.36e+02	2.03e+02	1.11e+02	8.26e+01	7.71e+01	7.46e+01
	Noise	2.93e+07	4.72e+06	7.76e+05	1.32e+05	2.34e+04	4.45e+03	9.48e+02	2.56e+02	1.14e+02	8.17e+01	7.69e+01	7.53e+01
	FGSM	2.50e+06	4.44e+05	9.49e+04	2.11e+04	4.89e+03	1.24e+03	3.66e+02	1.44e+02	9.01e+01	7.66e+01	7.53e+01	7.57e+01
	PGD	2.55e+06	4.38e+05	8.27e+04	1.87e+04	4.43e+03	1.13e+03	3.40e+02	1.39e+02	8.88e+01	7.66e+01	7.55e+01	7.60e+01
	SAWAR	1.31e+03	7.77e+02	4.72e+02	2.98e+02	1.98e+02	1.42e+02	1.10e+02	9.21e+01	8.28e+01	7.87e+01	7.80e+01	7.78e+01

TABLE VIII: Negative Log Likelihood metric for *SurvSet* datasets (lower is better) for each adversarial training method against the worst-case adversarial attack.